Thermodynamic Analysis of Binding between Mouse Major Urinary Protein-I and the Pheromone 2-*sec*-Butyl-4,5-dihydrothiazole†

Scott D. Sharrow, Milos V. Novotny,* and Martin J. Stone*

Department of Chemistry and Institute for Pheromone Research, Indiana University, Bloomington, Indiana 47405-0001

Received July 9, 2002; Revised Manuscript Received February 14, 2003

ABSTRACT: The mouse pheromone 2-*sec*-butyl-4,5-dihydrothiazole (SBT) binds to an occluded, nonpolar cavity in the mouse major urinary protein-I (MUP-I). The thermodynamics of this interaction have been characterized using isothermal titration calorimetry (ITC). MUP-I−SBT binding is accompanied by a large favorable enthalpy change ($\Delta H = -11.2$ kcal/mol at 25 °C), an unfavorable entropy change ($-T\Delta S = 2.8$ kcal/mol at 25 °C), and a negative heat capacity change [$\Delta C_p = -165$ cal/(mol K)]. Thermodynamic analysis of binding between MUP-I and several 2-alkyl-4,5-dihydrothiazole ligands indicated that the alkyl chain contributes more favorably to the enthalpy and less favorably to the entropy of binding than would be expected on the basis of the hydrophobic desolvation of short-chain alcohols. However, solvent transfer experiments indicated that desolvation of SBT is accompanied by a net unfavorable change in enthalpy ($\Delta H = +1.0$ kcal/mol) and favorable change in entropy ($-T\Delta S = -1.8$ kcal/mol). These results are discussed in terms of the possible physical origins of the binding thermodynamics, including (1) hydrophobic desolvation of both the protein and the ligand, (2) formation of a buried water-mediated hydrogen bond network between the protein and ligand, (3) formation of strong van der Waals interactions, and (4) changes in the structure, dynamics, and/or hydration of the protein upon binding.

Volatile pheromones (small molecules) have been implicated in mediating both endocrine responses and social behavior in house mice (*1*−*6*). These chemosignals are typically excreted in the urine and glandular secretions to stimulate highly specialized neurons (*7*) in the vomeronasal organ and the major olfactory epithelium of receiving conspecifics. Indeed, synthetic pheromones have proven biological activity in whole animals (*1*−*6*) and activity at neuronal membranes (*8*, *9*). During the chemosignaling function, the pheromones encounter different types of proteins: besides the G-protein-coupled receptor proteins (*7*, *10*, *11*), which are imbedded in the neuronal membrane, small (soluble) proteins in mucus have been postulated to participate in "perireceptor events" (*12*) as pheromone transporters, receptor-assisting proteins, or deactivating agents. However, the most studied pheromone-binding proteins are the so-called major urinary proteins (MUPs)[1] (*13*, *14*), a complex of protein isoforms encountered in mice and a structurally similar protein found in the Norway rat (*15*). MUPs appear to serve the function of slow-release and/or signal-modulating agents for the pheromones (*16*), although possible additional roles in chemosignaling have also been discussed recently (*17*).

This paper focuses on the physical basis of binding between the synthesized mouse pheromone, 2-*sec*-butyl-4,5-dihydrothiazole (SBT) or its several structural analogues, and one of the main MUP isoforms, MUP-I (Figure 1) prepared as a recombinant protein (*18*). SBT is a unique male pheromone which is involved in estrus synchrony, puberty acceleration, and attraction in females (*1*, *4*, *19*) and intermale aggression (*3*). Recent X-ray crystallography and NMR studies have provided information on the structures and dynamical properties of MUPs and their interactions with pheromones, including SBT (*18*, *20*−*23*). MUPs are members of the lipocalin family, which are related to the fatty acid-binding proteins (FABPs) and the avidins; together these three protein families constitute the calycin superfamily (*24*). The structure of the MUP-I−SBT complex (*22*) is shown in Figure 1C. Like other lipocalins, MUP-I consists of an eight-stranded antiparallel β-sheet with +1 connections (i.e., a β-meander). The terminal strands are hydrogen-bonded to each other so that the sheet forms a closed β-barrel. A short N-terminal 3_{10}-helix immediately preceding the first strand folds across one end of the barrel (top right in Figure 1C), and an Ω-loop, including turn-like structures, folds across the other end between the first two strands (bottom left in Figure 1C). The interior of the barrel consists of a hydrophobic cavity, which forms the binding site for ligands (*18*, *22*) and is completely occluded from solvent. The final secondary structural feature is a C-terminal α-helix, which packs against the outside of the β-barrel.

† This work was supported by grants awarded to M.J.S. from the National Science Foundation (MCB-9600968) and to M.V.N. from the National Institute of Deafness and Communication Disorders (DC 02418).

* To whom correspondence should be addressed. M.J.S.: phone, 812-855-6779; fax, 812-855-8300; e-mail, mastone@indiana.edu. M.V.N.: phone, 812-855-4532; fax, 812-855-8300; e-mail, novotny@indiana.edu.

[1] Abbreviations: ASA, accessible surface area; ET, 2-ethyl-4,5-dihydrothiazole; FABP, fatty acid-binding protein; IBT, 2-ethyl-4,5-dihydrothiazole; IPT, 2-isopropyl-4,5-dihydrothiazole; ITC, isothermal titration calorimetry; MT, 2-methyl-4,5-dihydrothiazole; MUP, mouse major urinary protein; pOBP, porcine odorant-binding protein; PT, 2-*n*-propyl-4,5-dihydrothiazole; SBT, 2-*sec*-butyl-4,5-dihydrothiazole.

10.1021/bi026423q CCC: $25.00
Published on Web 04/24/2003

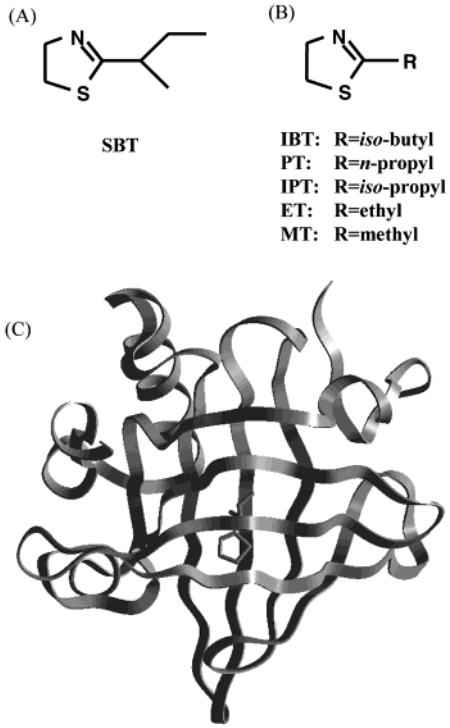

FIGURE 1: (A) Structure of 2-*sec*-butyl-4,5-dihydrothiazole (SBT). (B) Structures and abbreviations of the other 2-alkyl-4,5-dihydrothiazoles used in this study. (C) Structure of the MUP-I−SBT complex (PDB accession code 1I06). MUP-I is represented as a ribbon, and SBT (located in the central cavity of MUP-I) is represented as solid cylinders.

SBT binds into the interior hydrophobic cavity of MUP-I with a dissociation equilibrium constant (K_d) of ~1 μM and stoichiometry of 1:1 (*18*). Approximately 86% of the protein and ligand surface area buried in this interaction is nonpolar, suggesting that the classical hydrophobic effect (a predominantly entropic effect) may make a substantial favorable contribution to the binding free energy. Furthermore, an NMR relaxation study of MUP-I in the presence and absence of SBT indicated that the backbone flexibility of MUP-I increases upon binding, suggesting that increased backbone conformational entropy also contributes favorably to binding affinity (*23*). On the other hand, the X-ray structure of the MUP-I−SBT complex revealed two buried water molecules apparently participating in a network of hydrogen bonds, bridging one of the heteroatoms of SBT (presumably the nitrogen) to several backbone and side chain groups in the protein (*22*). The structure of MUP-I bound to an unrelated pheromone (*22*) contained the same two water molecules, suggesting that the hydrogen bond network makes an important (enthalpic) contribution to the binding affinity.

These previous observations prompted us to undertake the study of MUP-I−SBT binding thermodynamics described herein. Initial experiments indicated that binding is enthalpically favorable and entropically unfavorable. To investigate whether the classical hydrophobic effect makes a significant contribution to binding, we determined the heat capacity change for MUP-I−SBT binding and also studied binding of MUP-I to a series of SBT analogues with different alkyl groups. The possible physical origin of the observed thermodynamic effects is discussed.

EXPERIMENTAL PROCEDURES

MUP-I Expression and Purification. MUP-I was expressed in *Escherichia coli* and purified as described (*18*), with the minor modification that the nickel-affinity (His-Bind; Novagen, Madison, WI) chromatographic step was implemented a second time on the factor Xa cleavage products to remove uncleaved fusion protein from the released protein.

Ligand Synthesis and Analysis. 2-*sec*-Butyl-4,5-dihydrothiazole (SBT), 2-*n*-propyl-4,5-dihydrothiazole (PT), and 2-isopropyl-4,5-dihydrothiazole (IPT) were available from stocks previously prepared in our laboratory using published methods (*18*, *25*). 2-Methyl-4,5-dihydrothiazole (MT) was purchased from Aldrich Chemical Co. (Milwaukee, WI).

Isobutyl-4,5-dihydrothiazole (IBT) was prepared as follows. Hexamethyldisilazane (10.6 mL, 8.1 g, 50 mmol) and 2-aminoethanol (6.03 mL, 6.1 g, 100 mmol) were heated together for 3 h using a 100 °C bath. The fraction containing 2-trimethylsilyloxyethylamine (bp 130−135 °C) was collected by distillation, then diluted to 2 M final concentration in chloroform, and cooled in an ice bath. One equivalent of 3-methylbutanoyl chloride (prepared by slowly adding a 5% excess of thionyl chloride to 2-methylbutyric acid and heating for 1 h in a 70 °C bath) was slowly added, then the mixture was warmed to room temperature, and the chloroform was removed by rotary evaporation. The product was extracted with ether, while inorganic salts were removed by filtration. After removal of the ether, the residue [containing *N*-(2-trimethylsilyloxyethyl)-3-methylbutanoylamide] was diluted to a concentration of ~2 M in toluene and combined with 0.5 equiv of Lawesson's reagent. The mixture was heated under nitrogen for 4 h at 100 °C, washed with sodium bicarbonate, and dried over magnesium sulfate. The toluene was removed and the product (isobutyl-4,5-dihydrothiazole) purified by fractional distillation (bp 90−95 °C): ^{1}H NMR (300 MHz, $CDCl_3$) δ 4.17 (t, J = 8.1 Hz, 2H, H4 or H5), 3.24 (t, J = 8.1 Hz, 2H, H5 or H4), 2.03 (d, J = 6.6 Hz, 2H, H6), 1.96 (h, J = 6.6 Hz, 1H, H7), 0.937 (d, J = 6.6 Hz, 6H, H8).

Ethyl-4,5-dihydrothiazole (ET) was prepared as follows. To methyl-4,5-dihydrothiazole (1.47 mL, 15.4 mmol) in dry tetrahydrofuran under nitrogen at −78 °C was slowly added butyllithium (8 mL, 16.0 mmol). After 1.5 h of stirring at −78 °C, iodomethane (1 mL, 16.0 mmol) was added, and the mixture was stirred for another 30 min at −78 °C. The reaction was warmed to room temperature, quenched with ice (~5 g), extracted with methylene chloride, washed with brine, and dried over magnesium sulfate. The product was purified by fractional distillation (bp 87−92 °C): ^{1}H NMR (400 MHz, $CDCl_3$) δ 4.18 (t, J = 8.1 Hz, 2H, H4 or H5), 3.25 (t, J = 8.1 Hz, 2H, H5 or H4), 2.5 (q, J = 7.5 Hz, 2H, H6), 1.19 (t, J = 7.5 Hz, 3H, H7).

^{1}H NMR spectra of all six ligands were consistent with expectation. In addition, the purity of each sample was assessed using gas chromatography−mass spectrometry (GC-MS) performed using a Hewlett-Packard Series II 5890/5971 GC-MS system equipped with a Restec REX 5 capillary column (0.32 mm × 60 m, 0.5 μm film thickness). Samples were prepared by diluting 0.5 μL of each compound with 100 μL of ether. One microliter was injected and separated using a thermal gradient of 60−220 °C over 16 min; the injection port was held at 250 °C. GC-MS analyses indicated

that all samples were >97% pure.

Isothermal Titration Calorimetry. Isothermal titration calorimetry was carried out using a Microcal MCS instrument located at the Keck Biophysics Facility, Northwestern University, Evanston, IL. Samples of MUP protein (2.4 mL of 13−500 μM protein in 10 mM phosphate and 0.02% NaN_3, pH 6.3) were titrated with one 2 μL aliquot and then fifteen 4 μL aliquots of the pheromone or its analogue (0.01−2.6 mM in the same buffer). The duration of each injection was ~20 s, with a 210 s recovery time between injections. Titrations were performed at 20, 25, 30, and 35 °C. The reference cell was filled with distilled water. To account for heats of dilution and mechanical mixing, control titrations were performed by injection of the ligand into buffer; binding data were corrected by subtraction of the dilution data prior to curve fitting. Corrected binding data were processed using the Origin ITC analysis software package supplied by Microcal (Northampton, MA). The data were fit well to the following equation (*26*), describing the cumulative heat (Q) evolved from a series of injections when the ligand (L) binds to a set of identical, independent binding sites on the protein (P):

$$Q = 1 + [\mathrm{P}]_{\mathrm{total}} n K_{\mathrm{a}} + K_{\mathrm{a}}[\mathrm{L}]_{\mathrm{total}} - \{[(1 + [\mathrm{P}]_{\mathrm{total}} n K_{\mathrm{a}} + K_{\mathrm{a}}[\mathrm{L}]_{\mathrm{total}})^2 - 4[\mathrm{P}]_{\mathrm{total}} n K_{\mathrm{a}}^2 [\mathrm{L}]_{\mathrm{total}}]^{1/2} (2K_{\mathrm{a}}/V\Delta H^\circ)\}$$

in which V represents the initial reaction volume. Nonlinear curve fitting of the first derivative of Q with respect to $[\mathrm{L}]_{\mathrm{total}}$ plotted against the molar ratio of ($[\mathrm{L}]_{\mathrm{total}}/[\mathrm{P}]_{\mathrm{total}}$) yielded the association equilibrium constant ($K_{\mathrm{a}} = 1/K_{\mathrm{d}}$), the binding stoichiometry (n = number of ligand binding sites per protein molecule), and the enthalpy of binding (ΔH°).

Solvent Transfer Experiments. The apparent equilibrium constant for partitioning between water and cyclohexane ($K_{\mathrm{p,app}} = [\mathrm{SBT}]_{\mathrm{tot,ch}}/[\mathrm{SBT}]_{\mathrm{w}}$; subscripts tot, ch, and w refer to total, cyclohexane, and water, respectively) was determined from solvent partitioning experiments (monitored using capillary gas chromatography) with varying total concentrations of SBT (*27*). The equilibrium constant for solvation of SBT in cyclohexane ($K_{\mathrm{h}} = [\mathrm{SBT}{-}\mathrm{H_2O}]_{\mathrm{ch}}/[\mathrm{SBT}]_{\mathrm{free,ch}}[\mathrm{H_2O}]_{\mathrm{free,ch}}$) was obtained by monitoring the ability of increasing SBT concentrations to induce transfer of $^3\mathrm{H_2O}$ into cyclohexane (*27*). The corrected equilibrium constant for partitioning between water and cycohexane ($K_{\mathrm{p,corr}} = [\mathrm{SBT}]_{\mathrm{free,ch}}/[\mathrm{SBT}]_{\mathrm{w}}$) was calculated as $K_{\mathrm{p,corr}} = K_{\mathrm{p,app}}/(1 + K_{\mathrm{h}}[\mathrm{H_2O}]_{\mathrm{ch}})$, and the free energy of transfer of SBT from water to cyclohexane was then calculated as $\Delta G_{\mathrm{p}} = -RT \ln[K_{\mathrm{p,corr}}(\upsilon_{\mathrm{cyclohexane}}/\upsilon_{\mathrm{wat}})]$, in which R is the gas constant, T is the absolute temperature, and $\upsilon_{\mathrm{cyclohexane}}/\upsilon_{\mathrm{wat}}$ is the ratio of the molar volumes of cyclohexane and water (*27*, *28*). Further details of these experiments are given in the Supporting Information.

Structural Modeling and Surface Area Calculations. The coordinates for the MUP-I−SBT complex were obtained from Protein Data Bank entry 1I06. Models of MUP-I or its complexes for surface area calculations were built using the program Insight II (Molecular Simulations, Inc., San Diego, CA). All water molecules except the two involved in the protein−ligand hydrogen bond network (W507 and W512) were removed. Models with *n*-propyl, isopropyl, ethyl, or methyl analogues of SBT were obtained by removing the appropriate carbon atoms from SBT. The model with the isobutyl ligand was obtained by adding a methyl group to the appropriate carbon of the *n*-propyl analogue. A model of free SBT, with the two water molecules, was obtained by removal of the ligand. The apolar accessible surface areas in the various models were determined with the program Naccess (version 2.1; S. J. Hubbard, Biomolecular Structure and Modeling Unit, University College, London, U.K.), using a solvent radius of 1.4 Å and a slice width of 0.25 Å and excluding hydrogen atoms.

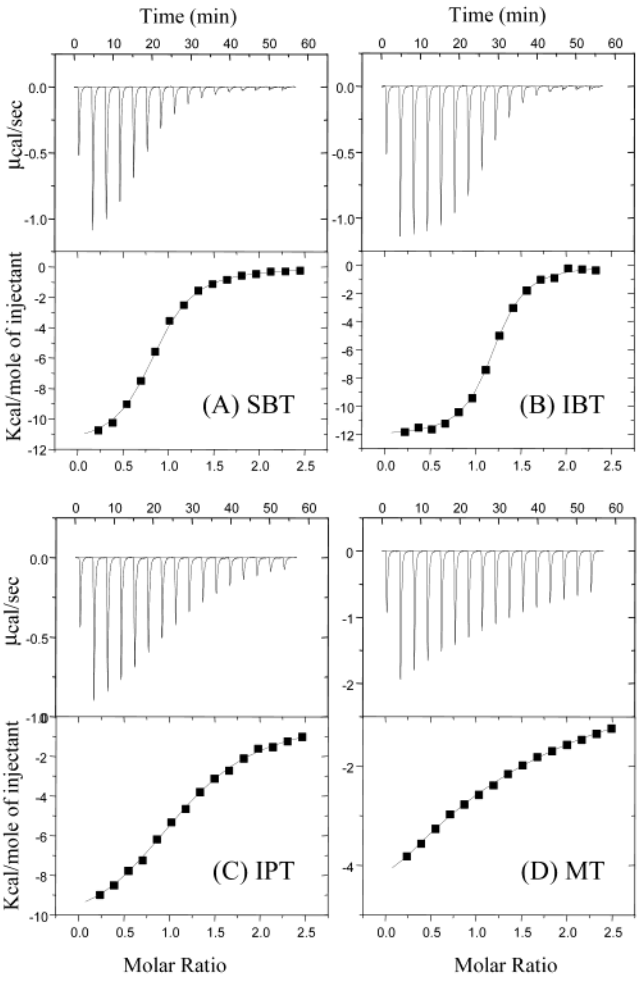

FIGURE 2: Isothermal titration calorimetry thermograms (upper panels) and fitted binding isotherms (lower panels) for binding at 25 °C of MUP-I to (A) SBT, (B) IBT, (C) IPT, and (D) MT.

RESULTS

Thermodynamics of MUP-I−SBT Binding by Titration Calorimetry. The thermodynamics of the interaction between MUP-I and SBT were studied by isothermal titration calorimetry (ITC). The ITC data at 25 °C are shown in Figure 2A. The thermogram (Figure 2A, upper panel) is of high quality, with an excellent signal-to-noise ratio and a stable baseline. The negative peaks indicate that the interaction is exothermic ($\Delta H < 0$). The integrated peak areas fit well to a standard binding isotherm, as evidenced by the excellent agreement between measured values and the fitted curve (Figure 2A, lower panel). The fitted thermodynamic parameters are listed in Table 1. The dissociation constant (K_{d}) is 0.74 ± 0.04 μM at 25 °C, which is in reasonable agreement

Table 1: Thermodynamic Parameters for MUP-I Binding to 2-Alkyl-4,5-dihydrothiazoles[a]

ligand	temp (°C)	K_d (μM)	stoichiometry (n)	ΔH (kcal/mol)	ΔS [cal/(mol K)]	ΔG (kcal/mol)	ΔC_p [cal/(mol K)]
SBT	21.6	0.56	0.800	−10.64	−7.5	−8.44	
	25.6	0.74	0.783	−11.2	−9.3	−8.38	
	30.2	0.96	0.822	−11.9	−11.7	−8.35	
	35.2	1.45	0.797	−12.9	−15.1	−8.23	
							−165 ± 9
IBT	20.7	0.19	1.134	−11.60	−8.6	−9.07	
	25.7	0.24	1.180	−11.90	−9.6	−9.04	
	30.5	0.34	1.151	−12.19	−10.6	−8.98	
	35.3	0.53	1.220	−12.39	−11.5	−8.85	
							−56 ± 6
PT	21.2	0.81	1.076	−10.62	−8.3	−8.20	
	25.5	1.06	1.079	−10.7	−8.7	−8.16	
	30.7	1.49	1.147	−10.97	−9.5	−8.09	
	35.5	2.6	1.167	−11.3	−11.0	−7.90	
							−53 ± 3
IPT	21.1	1.64	1.069	−10.5	−9.3	−7.79	
	25.4	1.9	0.97	−10.8	−10.2	−7.81	
	30.5	3.1	1.14	−11.5	−12.6	−7.65	
	35.0	5.0	1.16	−12.0	−15	−7.47	
							−111 ± 9
ET	20.8	6.5	1.033	−9.91	−10.0	−6.98	
	25.4	8.5	0.818	−10.00	−10.3	−6.93	
	30.3	13.3	1.208	−10.42	−12.0	−6.77	
	35.3	18.9	0.754	−10.5	−12.4	−6.67	
							−45 ± 9
MT	20.7	49	1.07	−8.9	−10.7	−5.79	
	25.3	78	1.04	−9.7	−14	−5.61	
	30.3	101	1.06	−10.3	−16	−5.55	
	35.3	147	1.1	−11	−18	−5.41	
							−134 ± 124

[a] MUP-I−SBT binding was measured three times at 25 °C, with excellent reproducibility, whereas the other values are from single measurements. Temperatures vary slightly between ligands. Listed temperatures are the actual temperatures at which the samples were equilibrated rather than the target temperatures. For most ligands, fitted errors in K_d, n, ΔH, ΔS, and ΔG values are ≤5%, ≤2%,≤3%,≤5%, and ≤5%, respectively. For MT, the errors in these parameters are as high as 9%, 11%, 14%, 30%, and 11%, respectively.

with the reported value of 1.3 ± 0.3 μM determined at 20 °C using an equilibrium diffusion assay (*18*). Similarly, the fitted binding stoichiometry (racemic ligand:protein ratio) is 0.783 ± 0.006, close to the value of 1.0 ± 0.1 determined by both NMR titration and the diffusion assay (*18*). It is noteworthy that both enantiomers of SBT bind to MUP-I with close to identical affinities (*18*).

The enthalpy of binding determined by ITC is $\Delta H = -11.2 \pm 0.1$ kcal/mol, and the total free energy change [$\Delta G = RT \ln(K_d)$, in which R is the universal gas constant] is −8.38 ± 0.02 kcal/mol. Consequently, the entropy contribution to binding [$-T\Delta S = \Delta G - \Delta H$] is 2.8 ± 0.1 kcal/mol at 25 °C, so that $\Delta S = -9.3 \pm 0.4$ cal/(mol K). These data indicate that the net binding free energy is dominated by a negative (favorable) enthalpy contribution and that the net entropy change is small and unfavorable ($\Delta S < 0$).

Influence of Buffer on Binding Thermodynamics. It has been noted previously that thermodynamic parameters measured by isothermal titration calorimetry can be influenced by the choice of buffer if either protonation or deprotonation accompanies the binding event of interest (*29*). If this is the case, the measured enthalpy of binding is expected to be linearly related to the intrinsic ionization enthalpy of the buffer, with the proportionality constant being the number of protons transferred upon binding (*29*). To investigate whether this effect was occurring in the MUP-I−SBT system, we measured the thermodynamics of MUP-I−SBT binding by ITC in five buffers whose ionization enthalpies vary over the range −0.05 to +7.51 kcal/mol. The thermodynamic binding parameters are identical within experimental error for all buffers. The independence of ΔH from the buffer ionization enthalpy (Table 2) indicates that binding is not coupled to protonation or deprotonation. This is structurally reasonable because there are no ionizable groups in the MUP-I binding cavity with pK_a values close to the experimental pH (6.3). The pK_a of the dihydrothiazole ring nitrogen is estimated to be ∼5.2 (*30*), suggesting that it is more than 90% deprotonated (uncharged) under the experimental conditions.

Table 2: Independence of MUP-I−SBT Apparent Binding Enthalpy from the Buffer Ionization Enthalpy[a]

buffer	ΔH_{ion} (kcal/mol)[b]	ΔH_{obs} (kcal/mol)[b]
cacodylate	−0.047	−12.3 ± 0.5
phosphate	1.22	−12.3 ± 0.3
PIPES	2.74	−12.6 ± 0.2
MES	3.71	−12.3 ± 0.4
ACES	7.51	−12.4 ± 0.2

[a] All data were determined by ITC at pH 6.3 and 30 °C. [b] ΔH_{ion} is the ionization enthalpy of the buffer; ΔH_{obs} is the observed binding enthalpy.

Temperature Dependence of MUP-I−SBT Binding Thermodynamics. SBT is predominantly hydrophobic, suggesting that the classical hydrophobic effect (the release of ordered water from the protein and ligand surfaces upon association) may contribute to the binding affinity. The thermodynamic hallmarks of the classical hydrophobic effect are a positive entropy change (due to the increased solvent disorder) and

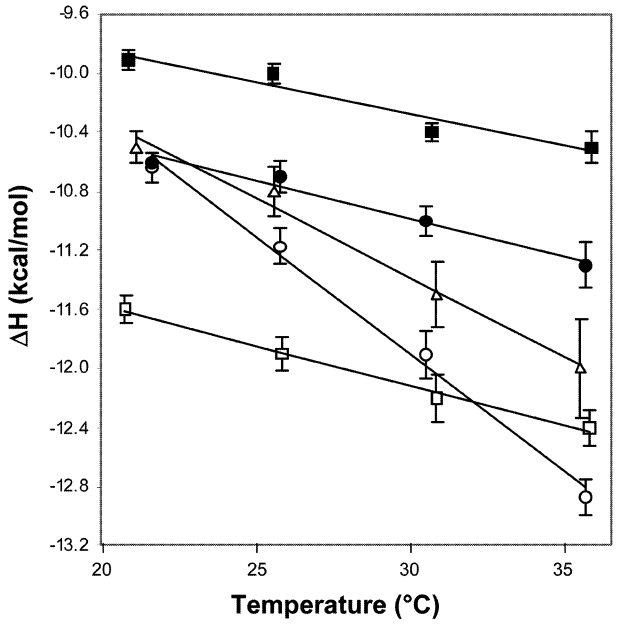

FIGURE 3: Temperature dependence of ΔH for binding of MUP-I to SBT (open circles), IBT (open squares), IPT (open triangles), PT (filled circles), and ET (filled squares). Data for MT are not included because error bars for this ligand are too large for reliable determination of ΔC_p.

a large negative change in heat capacity (due to the higher heat capacity of ordered water clusters relative to bulk water) (*31*−*35*). The small negative net entropy change for the MUP-I−SBT interaction could potentially be the sum of a positive contribution from hydrophobic desolvation, a negative contribution from the loss of rotational and translational entropy, and changes in internal conformational entropy. Thus, to probe the importance of the hydrophobic effect, we determined the change in heat capacity (ΔC_p) upon binding by repeating the ITC measurement of ΔH at several temperatures (see Table 1). A plot of ΔH versus temperature (Figure 3) is linear ($r^2 = 0.99$) with a slope [$\Delta C_p = \mathrm{d}(\Delta H)/\mathrm{d}T$] of -165 ± 9 cal/(mol K). This negative heat capacity is consistent with the proposal that the classical hydrophobic effect contributes to the binding free energy of the MUP-I−SBT complex.

Structural Partitioning of Thermodynamic Effects Using Ligand Analogues. Insights into the structural origin of the observed binding thermodynamics can potentially be obtained by comparing the binding thermodynamics of ligand and/or protein analogues. To investigate the thermodynamic contribution of the *sec*-butyl chain, we have studied the MUP-I binding of five analogues of SBT in which the *sec*-butyl group is replaced by isobutyl, *n*-propyl, isopropyl, ethyl, and methyl groups (labeled IBT, PT, IPT, ET, and MT, respectively; Figure 1B). The thermodynamic parameters for binding of these analogues to MUP-I at each of four temperatures are listed in Table 1, and graphs of ΔH versus temperature are shown in Figure 3. ITC thermograms and fitted binding isotherms for IBT, IPT, and MT are shown in Figure 2. The ITC data are of similar quality to the SBT data, and in all cases the binding stoichiometry is close to 1:1. The shorter chain analogues bind more weakly than the *sec*-butyl and isobutyl compounds, with the K_d increasing by ~100-fold from butyl to methyl compounds. As discussed below, the reduction in affinity for thiazole ligands with shorter alkyl chains has both enthalpic and entropic components. Interestingly, the ΔC_p values for the two C6-branched ligands, SBT [-165 ± 9 cal/(mol K)] and IPT [-111 ± 9 cal/(mol K)], are dramatically more negative than those of the other ligands [−40 to −60 cal/(mol K) for IBT, PT, and ET]; the value for MT was poorly determined.

Thermodynamics of SBT Transfer from Water to Cyclohexane. The thermodynamics of MUP-I−SBT binding can be conceptually partitioned into (1) the thermodynamics associated with desolvation of SBT, (2) the thermodynamics associated with desolvation of the binding cavity, (3) the new interactions that form between the protein and ligand, and (4) internal structural rearrangements of the protein and/or ligand. The first two terms include any changes in solvent−solvent interactions or solvent entropy that accompany desolvation. To estimate the contribution of ligand desolvation to MUP-I−SBT binding, we measured the thermodynamics of transferring SBT from water to cyclohexane using classical solvent partitioning experiments. The choice of cyclohexane rather than another organic solvent was guided by the previous observation that there is a good correlation between the cyclohexane to water transfer free energies of the amino acids and their relative accessibility in proteins (*36*). Nevertheless, a caveat of this approach is that no individual solvent is necessarily an accurate mimic of the interior environment of MUP-I (or any other protein).

A series of transfer experiments was performed at each of several temperatures for each of several total concentrations of SBT. A plot of aqueous versus organic concentrations of SBT (Figure 4A) shows excellent linearity as the concentration of SBT is varied at 25 °C. The slopes of this graph and similar graphs for the data at other temperatures yielded the apparent equilibrium partitioning coefficients ($K_{p,app}$) listed in Table 3 (*27*).

The $K_{p,app}$ values reflect the equilibrium between the total SBT concentration in the aqueous phase and the total SBT concentration in the cyclohexane phase. However, since we are interested in the energetics of desolvation, it is imperative to know the concentrations of fully solvated SBT (in the aqueous phase) and fully desolvated SBT (in the organic phase). It is reasonable to assume that essentially all of the

Table 3: Thermodynamics of SBT Transfer from Water to Cyclohexane[a]

	20 °C	25 °C	30 °C	35 °C
$K_{p,app}$	4.0 ± 0.1	4.1 ± 0.09	4.3 ± 0.1	4.4 ± 0.07
K_h (M^{-1})	23 ± 1	19 ± 1	15 ± 2	13 ± 3
$K_{p,corr}$	3.8 ± 0.1	3.9 ± 0.1	4.0 ± 0.2	4.1 ± 0.1
ΔG_p (kcal/mol)	−0.78 ± 0.02	−0.80 ± 0.02	−0.84 ± 0.03	−0.87 ± 0.02

[a] $K_{p,app}$, apparent equilibrium constant for transfer of SBT from water to cyclohexane; K_h, equilibrium constant for hydration of SBT in cyclohexane; $K_{p,corr}$, corrected equilibrium constant for transfer of SBT from water to cyclohexane; ΔG_p, mole fraction of free energy of transfer. Details of the experimental methods and data analysis are given in the Supporting Information.

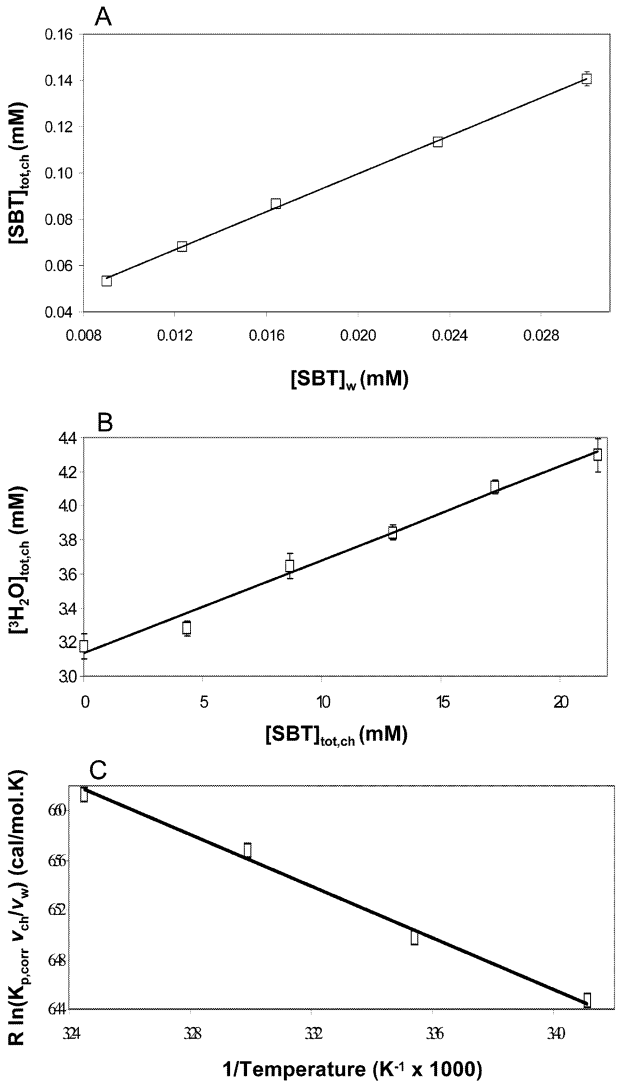

FIGURE 4: Thermodynamics of transfer of SBT from water to cyclohexane. (A) Equilibrium concentrations of SBT in cyclohexane ($[SBT]_{tot,ch}$) versus in water ($[SBT]_w$) at 25 °C for various total concentrations of SBT. The slope of this graph is the apparent partitioning coefficient ($K_{p,app}$). (B) Concentration of tritiated water in the cyclohexane phase ($[^3H_2O]_{tot,ch}$) plotted against the total SBT concentration in cyclohexane ($[SBT]_{tot,ch}$). Fitting of this curve yielded the solubility of water in cyclohexane and the equilibrium constant for hydration of SBT in cyclohexane. (C) van't Hoff plot for the transfer of SBT from water to cyclohexane. The ratio of the molar volumes of cyclohexane and water (v_{ch}/v_w) is included to convert the concentration units to mole fraction. Details of the experimental methods and data analysis are given in the Supporting Information.

aqueous SBT is solvated. However, a significant proportion of the SBT in the organic phase could potentially be associated with water, due to the intrinsic solubility of water in cyclohexane or the possibility that SBT selectively associates with water, thus increasing the effective concentration of water in cyclohexane. To correct for this possibility, we applied the method of Wimley and White (*27*), in which solvent-phase association of the ligand with water is revealed by the ability of the ligand to induce transfer of tritiated water into the organic phase. A plot of ^3H_2O concentration versus total SBT concentration in the solvent phase at 25 °C is linear (Figure 4B). This and similar plots for the other temperatures yielded the values of the hydration equilibrium constant of SBT in cyclohexane (K_h) listed in Table 3. This analysis also

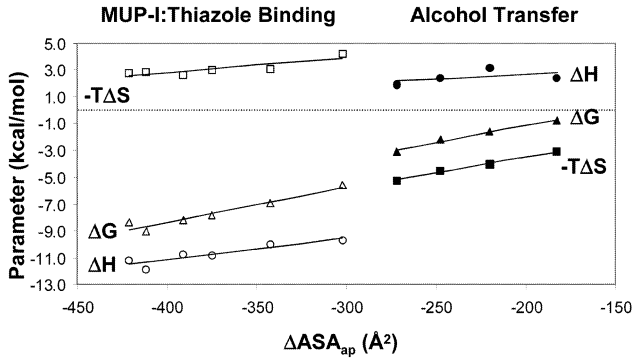

FIGURE 5: Dependence of thermodynamic parameters on the change in apolar accessible surface area (ΔASA_{ap}) for the binding of 2-alkyl-4,5-dihydrothiazoles to MUP-I (left side) and the transfer of *n*-alcohols from water to the neat organic phase (right side).

indicated that the solubility of water in cyclohexane is 3.1 mM at 25 °C, in excellent agreement with previous reported values (*27*).

Using the data for ligand solvation in cyclohexane, we determined corrected equilibrium partitioning coefficients ($K_{p,corr}$) and the corresponding mole fraction transfer (partitioning) free energy values (Table 3). The van't Hoff plot for these data (Figure 4C) is linear ($r^2 = 0.99$) and yields $\Delta H_p = +1.0$ kcal/mol and $\Delta S_p = +6.2$ cal/(mol K) (within the temperature range 20−35 °C). In summary, at 25 °C, the transfer of SBT from water to solvent is a favorable process ($\Delta G = -0.80$ kcal/mol), dominated by a favorable change in entropy ($-T\Delta S = -1.8$ kcal/mol) with an unfavorable enthalpic contribution.

DISCUSSION

The data presented above indicate that binding of MUP-I to SBT is characterized by a favorable enthalpy change, an unfavorable entropy change, and a negative change in heat capacity. In an effort to separate the thermodynamic contribution of the *sec*-butyl chain, we have measured the thermodynamics of MUP-I binding for several SBT analogues with different alkyl chains. Figure 5 shows the dependence of the thermodynamic parameters (ΔG, ΔH, and $-T\Delta S$) at 25 °C on the estimated change in accessible apolar surface area upon binding (ΔASA_{ap}) for each complex. This graph indicates that the increase in affinity for the longer chain ligands contains both enthalpic and entropic contributions with the enthalpic component [16 cal/(mol Å^2)] being about 50% larger than the entropic component [11 cal/(mol Å^2)]; the slope of the free energy curve is 26 cal/(mol Å^2). The ΔASA_{ap} values used in this analysis were calculated under the assumptions that (1) the position and orientation of each SBT analogue in the MUP-I binding site are close to those observed for SBT in the MUP-I−SBT crystal structure and (2) the MUP-I structure does not change significantly upon binding the various ligands. Variations in the structural details of the various complexes would introduce errors into the surface area changes in Figure 5. On the other hand, the incremental changes in thermodynamic parameters obtained here will not be influenced by consistent differences between the free and bound structures of MUP-I because the free structure is the same in all cases.

For comparison with the incremental thermodynamic terms expected for classical hydrophobic interactions, we also

present (Figure 5) thermodynamic data for the transfer of short-chain alcohols from aqueous to neat alcohol phases at 25 °C (*37*). There is a clear contrast between the thermodynamics of alcohol transfer and those of MUP-I−ligand binding. First, the alcohol transfer is entropically driven ($-T\Delta S < 0$ and $\Delta H > 0$) whereas the MUP-I binding is dominated by a favorable enthalpy change ($\Delta H < 0$ and $-T\Delta S > 0$). Second, and more importantly, the incremental change in enthalpy for alcohol transfer [6 cal/(mol Å^2)] is 2.7-fold less favorable than that for MUP-I−thiazole binding, whereas the incremental change in entropy for alcohol transfer [24 cal/(mol Å^2)] is 2.1-fold more favorable than that for MUP-I−thiazole binding. The compensating nature of these changes results in a similar dependence of ΔG on surface area burial [25 cal/(mol Å^2)].

The comparison of Figure 5 indicates that the favorable enthalpic contribution of the *sec*-butyl chain is unlikely to result purely from classical hydrophobic desolvation. However, some component of this favorable enthalpy may arise from desolvation of the protein and/or the ligand. Using solvent transfer experiments, we found that desolvation of SBT is only slightly unfavorable enthalpically ($\Delta H = +1.0$ kcal/mol). Considering that desolvation of the polar atoms in the thiazole moiety is expected to be enthalpically strongly disfavored, it appears that desolvation of the hydrophobic portion of the ligand may, in fact, be enthalpically favorable, analogous to the situation for alcohol transfer (Figure 5). Further evidence for this proposal would require extensive solvent transfer experiments with the different ligands.

Although the above analysis suggests that burial of the *sec*-butyl chain makes a significant contribution to the enthalpy of MUP-I−SBT binding, the magnitude of this contribution is somewhat smaller than the total binding enthalpy (−11.2 kcal/mol). This suggests that here is a common component of all MUP-I−thiazole complexes that contributes favorable enthalpy to the binding interactions. An obvious candidate is the network of water-mediated hydrogen bonds observed in the MUP-I−SBT crystal structure (*22*). Direct confirmation of the role of this hydrogen bond network would require analysis of ligand or protein analogues specifically designed to disrupt the network.

There are a number of previous reports of systems in which binding of nonpolar ligands to deep clefts or occluded cavities in proteins is driven by a favorable enthalpy change. Of particular relevance to the current system, binding of the "bell pepper"-odorant 2-isobutyl-3-methoxypyrazine or of 3,7-dimethyloctan-1-ol to the buried cavity of the lipocalin porcine odorant-binding protein (pOBP) is accompanied by a large favorable change in enthalpy ($\Delta H = -23.2$ and −21.0 kcal/mol, respectively, at pH 6.6) and a large unfavorable decrease in entropy ($-T\Delta S = 14.0$ and 11.5 kcal/mol, respectively, at pH 6.6) (*38*). Binding of acyl-CoA esters to the acyl-CoA binding protein (a four-helix bundle protein with a bowl-shaped binding cleft) involves favorable changes in both enthalpy and entropy (*39*). As the acyl chain length is increased, the enthalpy change becomes significantly more favorable (by 0.46 kcal/mol per CH_2 group), indicating that the interactions of the hydrocarbon portions of the ligand account for an important part of the binding enthalpy, as observed here. In both of these previous cases, there is no evidence for substantial structural transitions upon binding, and the authors attributed the favorable enthalpy changes to van der Waals interactions. In contrast, binding of myristoyl-CoA analogues to myristoyl-CoA:protein *N*-myristoyltransferase (*40*) and binding of ligands to intestinal fatty acid-binding protein (*41*−*43*) are both enthalpically favorable and accompanied by disorder-to-order structural transitions of the relevant protein, suggesting that a significant part of the binding enthalpy arises from structure formation. In the case of MUP-I−SBT binding, NMR chemical shifts indicate that there is no dramatic structural change of MUP-I upon binding (*18*), and NMR relaxation measurements revealed a slight *increase* in MUP-I backbone flexibility when it binds to SBT (*23*). However, there are currently no data to indicate whether the protein side chains become more or less ordered upon binding, so a disorder-to-order transition of the side chains remains a possibility. Of course, any change in the structural ensemble of the protein could be accompanied by changes in protein solvation at positions distant from the binding cavity, which would further contribute to the binding thermodynamics.

Summary. The data reported herein show that binding of MUP-I to SBT is accompanied by a favorable enthalpy change, an unfavorable entropy change, and a negative change in heat capacity. Comparison of MUP-I binding by SBT analogues further indicates that the interactions of the *sec*-butyl chain are associated with favorable changes in both enthalpy and entropy. Among the physical effects that may contribute to these changes are (1) hydrophobic desolvation of both the protein and the ligand, (2) formation of a buried water-mediated hydrogen bond network between the protein and ligand, (3) formation of strong van der Waals interactions, and (4) changes in the structure, dynamics, and/or hydration of the protein upon binding. Additional biophysical experiments will be required to distinguish between these possibilities.

ACKNOWLEDGMENT

The authors thank Dr. Jeffrey Vaughn for critical reading of the manuscript. We acknowledge the use of instruments in the Keck Biophysics Facility at Northwestern University (http://x.biochem.nwu.edu/Keck/keckmain.html).

SUPPORTING INFORMATION AVAILABLE

Detailed experimental and data analysis methods for the solvent transfer experiments. This material is available free of charge via the Internet at http://pubs.acs.org.

REFERENCES

1. Jemiolo, B., Harvey, S., and Novotny, M. (1986) Promotion of the Whitten effect in female mice by synthetic analogues of male urinary constituents, *Proc. Natl. Acad. Sci. U.S.A 83*, 4576−4579.
2. Novotny, M. V., Ma, W., Zidek, L., and Daev, E. (1999) in *Advances in chemical communication in vertebrates* (Johnston, R. E., Muller-Schartze, D., and Sorensen, P., Eds.) Plenum Press, New York.
3. Novotny, M., Harvey, S., Jemiolo, B., and Alberts, J. (1985) Synthetic pheromones that promote inter-male aggression in mice, *Proc. Natl. Acad. Sci. U.S.A. 82*, 2059−2061.
4. Jemiolo, B., Alberts, J., Sochinski-Wiggins, S., Harvey, S., and Novotny, M. (1985) Behavioural and endocrine responses of female mice to synthetic analogues of volatile compounds in male urine, *Anim. Behav. 33*, 1114−1118.

5. Novotny, M., Jemiolo, B., Harvey, S., Wiesler, D., and Marchlewska-Koj, A. (1986) Adrenal-mediated endogenous metabolites inhibit puberty in female mice, *Science 231*, 722−725.
6. Ma, W., Miao, Z., and Novotny, M. V. (1999) Induction of estrus in grouped female mice (mus domesticus) by synthetic analogues of preputial gland constituents, *Chem. Senses 24*, 289−293.
7. Buck, L. B. (1992) The olfactory multigene family, *Curr. Opin. Neurobiol. 2*, 282−288.
8. Leinders-Zufall, T., Lane, A. P., Puche, A. C., Ma, W., Novotny, M. V., Shipley, M. T., and Zufall, F. (2000) Ultrasensitive pheromone detection by mammalian vomeronasal neurons, *Nature 405*, 792−796.
9. Sam, M., Vora, S., Malnic, B., Ma, W., Novotny, M. V., and Buck, L. B. (2001) Neuropharmacology. Odorants may arouse instinctive behaviours, *Nature 412*, 142.
10. Buck, L., and Axel, R. (1991) A novel multigene family may encode odorant receptors: a molecular basis for odor recognition, *Cell 65*, 175−187.
11. Wu, Y., Tirindelli, R., and Ryba, N. J. (1996) Evidence for different chemosensory signal transduction pathways in olfactory and vomeronasal neurons, *Biochem. Biophys. Res. Commun. 220*, 900−904.
12. Breer, H. (1994) Odor recognition and second messenger signaling in olfactory receptor neurons, *Semin. Cell Biol. 5*, 25−32.
13. Finlayson, J. S., Potter, M., and Runner, R. C. (1963) *J. Natl. Cancer Inst. 31*, 91−107.
14. al Shawi, R., Ghazal, P., Clark, A. J., and Bishop, J. O. (1989) Intraspecific evolution of a gene family coding for urinary proteins, *J. Mol. Evol. 29*, 302−313.
15. Bayard, C., Holmquist, L., and Vesterberg, O. (1996) Purification and identification of allergenic alpha (2u)-globulin species of rat urine, *Biochim. Biophys. Acta 1290*, 129−134.
16. Robertson, D. H. L., Hurst, J. L., Hubbard, S. J., Gaskell, S. J., and Beynon, R. J. (1998) Ligands of urinary lipocalins from the mouse: uptake of environmentally derived chemicals, *J. Chem. Ecol. 24*, 1127−1140.
17. Hurst, J. L., Payne, C. E., Nevison, C. M., Marie, A. D., Humphries, R. E., Robertson, D. H., Cavaggioni, A., and Beynon, R. J. (2001) Individual recognition in mice mediated by major urinary proteins, *Nature 414*, 631−634.
18. Zidek, L., Stone, M. J., Lato, S. M., Pagel, M. D., Miao, Z., Ellington, A. D., and Novotny, M. V. (1999) NMR mapping of the recombinant mouse major urinary protein I binding site occupied by the pheromone 2-*sec*-butyl-4,5-dihydrothiazole, *Biochemistry 38*, 9850−9861.
19. Novotny, M. V., Ma, W., Wiesler, D., and Zidek, L. (1999) Positive identification of the puberty-accelerating pheromone of the house mouse: the volatile ligands associating with the major urinary protein, *Proc. R. Soc. London, Ser. B 266*, 2017−2022.
20. Bocskei, Z., Groom, C. R., Flower, D. R., Wright, C. E., Phillips, S. E., Cavaggioni, A., Findlay, J. B., and North, A. C. (1992) Pheromone binding to two rodent urinary proteins revealed by X-ray crystallography, *Nature 360*, 186−188.
21. Lucke, C., Franzoni, L., Abbate, F., Lohr, F., Ferrari, E., Sorbi, R. T., Ruterjans, H., and Spisni, A. (1999) Solution structure of a recombinant mouse major urinary protein, *Eur. J. Biochem. 266*, 1210−1218.
22. Timm, D. E., Baker, L. J., Mueller, H., Zidek, L., and Novotny, M. V. (2001) Structural basis of pheromone binding to mouse major urinary protein (MUP-I), *Protein Sci. 10*, 997−1004.
23. Zidek, L., Novotny, M. V., and Stone, M. J. (1999) Increased protein backbone conformational entropy upon hydrophobic ligand binding, *Nat. Struct. Biol. 6*, 1118−1121.
24. Flower, D. R. (1996) The lipocalin protein family: structure and function, *Biochem J. 318* (Part 1), 1−14.
25. North, M., and Pattenden, G. (1990) Synthetic studies towards cyclic peptides. concise synthesis of thiazoline and thiazole containing amino acids, *Tetrahedron 46*, 8267−8290.
26. Holdgate, G. A. (2001) Making cool drugs hot: isothermal titration calorimetry as a tool to study binding energetics, *BioTechniques 31*, 164−166, 168, 170.
27. Wimley, W. C., and White, S. H. (1992) Partitioning of tryptophan side-chain analogues between water and cyclohexane, *Biochemistry 31*, 12813−12818.
28. Wimley, W. C., Creamer, T. P., and White, S. H. (1996) Solvation energies of amino acid side chains and backbone in a family of host−guest pentapeptides, *Biochemistry 35*, 5109−5124.
29. Gomez, J., and Freire, E. (1995) Thermodynamic mapping of the inhibitor site of the aspartic protease endothiapepsin, *J. Mol. Biol. 252*, 337−350.
30. Weinberger, M. A., and Greenhalgn, R. (1963) The nuclear magnetic resonance spectra of some 2-methyl-Δ2-oxazolines and 2-methyl-Δ2-thiazolines, *Can. J. Chem. 41*, 1038−1041.
31. Tanford, C. (1980) *The hydrophobic effect: formation of micelles and biological membranes*, John Wiley and Sons, New York.
32. Blokzijl, W., and Engberts, J. B. F. N. (1993) Hydrophobic effects: opinions and facts, *Angew. Chem., Int. Ed. Engl. 32*, 1545−1579.
33. Muller, N. (1990) Search for a realistic view of hydrophobic effects, *Acc. Chem. Res. 23*, 23−28.
34. Privalov, P. L., and Gill, S. J. (1988) Stability of protein structure and hydrophobic interaction, *Adv. Protein Chem. 39*, 191−234.
35. Spolar, R. S., and Record, M. T., Jr. (1994) Coupling of local folding to site-specific binding of proteins to DNA, *Science 263*, 777−784.
36. Radzicka, A., and Wolfenden, R. (1988) Comparing the polarities of the amino acids: side-chain distribution coefficients between the vapor phase, cyclohexane, 1-octanol, and neutral aqueous solution, *Biochemistry 27*, 1664−1670.
37. Arnett, E. M., Kover, W. B., and Carter, J. V. (1969) Heat capacities of organic compounds in solution. I. Low molecular weight alcohols in water, *J. Am. Chem. Soc. 91*, 4028−4034.
38. Burova, T. V., Choiset, Y., Jankowski, C. K., and Haertle, T. (1999) Conformational stability and binding properties of porcine odorant binding protein, *Biochemistry 38*, 15043−15051.
39. Faergeman, N. J., Sigurskjold, B. W., Kragelund, B. B., Andersen, K. V., and Knudsen, J. (1996) Thermodynamics of ligand binding to acyl-coenzyme A binding protein studied by titration calorimetry, *Biochemistry 35*, 14118−14126.
40. Bhatnagar, R. S., Jackson-Machelski, E., Mcwherter, C. A., and Gordon, J. I. (1994) Isothermal titration calorimetric studies of *Saccharomyces cerevisiae* myristoyl-CoA:protein N-myristoyltransferase. Determinants of binding energy and catalytic discrimination among acyl-CoA and peptide ligands, *J. Biol. Chem. 269*, 11045−11053.
41. Richieri, G. V., Ogata, R. T., and Kleinfeld, A. M. (1995) Thermodynamics of fatty acid binding to fatty acid-binding proteins and fatty acid partition between water and membranes measured using the fluorescent probe ADIFAB, *J. Biol. Chem. 270*, 15076−15084.
42. Hodsdon, M. E., and Cistola, D. P. (1997) Ligand binding alters the backbone mobility of intestinal fatty acid-binding protein as monitored by N-15 NMR relaxation and H-1 exchange, *Biochemistry 36*, 2278−2290.
43. Hodsdon, M. E., and Cistola, D. P. (1997) Discrete backbone disorder in the nuclear magnetic resonance structure of apo intestinal fatty acid-binding protein: implications for the mechanism of ligand entry, *Biochemistry 36*, 1450−1460.

BI026423Q